

# Higher Order Hierarchical Curved Hexahedral Vector Finite Elements for Electromagnetic Modeling

Milan M. Ilić, *Student Member, IEEE*, and Branislav M. Notaroš, *Member, IEEE*

**Abstract**—A novel higher order finite-element technique based on generalized curvilinear hexahedra with hierarchical curl-conforming polynomial vector basis functions is proposed for microwave modeling. The finite elements are implemented for geometrical orders from 1 to 4 and field-approximation orders from 1 to 10 in the same Galerkin-type finite-element method and applied to eigenvalue analysis of arbitrary electromagnetic cavities. Individual curved hexahedra in the model can be as large as approximately  $2\lambda \times 2\lambda \times 2\lambda$ , which is 20 times the traditional low-order modeling discretization limit of  $\lambda/10$  in each dimension. The examples show excellent flexibility and efficiency of the higher order (more precisely, low-to-high order) method at modeling of both field variation and geometrical curvature, and its excellent properties in the context of  $p$ -refinement of solutions, for models with both flat and curved surfaces. The reduction in the number of unknowns is by an order of magnitude when compared to low-order solutions.

**Index Terms**—Cavities, computer-aided analysis, electromagnetic analysis, finite-element methods (FEMs).

## I. INTRODUCTION

THE finite-element method (FEM) for discretizing partial differential equations in electromagnetics is an extremely powerful and versatile general numerical methodology for electromagnetic-field simulation in RF and microwave applications [1]–[20]. However, practically all the existing three-dimensional (3-D) FEM electromagnetic tools are low-order (subdomain) techniques—the electromagnetic structure is modeled by volume geometrical elements that are electrically very small and the fields within the elements are approximated by low-order (zeroth- and first-order) basis functions. More precisely, the elements are on the order of  $\lambda/10$  in each dimension,  $\lambda$  being the wavelength in the medium, in both closed-region (e.g., waveguide/cavity) and open-region (e.g., antenna/scattering) problems. This results in a very large number of unknowns (unknown field-distribution coefficients) needed to obtain results of satisfactory accuracy, with all the associated problems and enormous requirements in computational resources. In addition, commonly used 3-D elements are in the form of bricks, tetrahedra, and triangular prisms, all with planar sides, and, thus, they do not provide enough flexibility and efficiency in modeling of structures with pronounced curvature.

An alternative that can greatly reduce the number of unknowns for a given problem and enhance further the accuracy and efficiency of the FEM analysis in all classes of applications is the higher order (or large-domain) computational approach. This approach utilizes higher order basis functions defined in large geometrical elements (e.g., on the order of  $\lambda$  in each dimension). Only relatively recently the computational electromagnetics (CEM) community has started to extensively investigate and employ higher order finite elements and higher order basis functions [7]–[17]. Higher order electromagnetic modeling is definitely becoming the mainstream of activity in CEM. However, although several types of geometrical elements and basis functions of arbitrarily high orders have been proposed and described [2], [7], [10], [15], [17], [18], almost none of the reported results and applications demonstrate actual use and implementation of models of orders higher than two. Notable examples of higher order FEM modeling are hierarchical vector elements proposed in [15] and [16], where elements in the form of tetrahedra with field-approximation basis functions of up to the fourth order are demonstrated, and interpolatory vector elements proposed in [8], where third-order elements are implemented in both tetrahedral and hexahedral forms. In addition, it seems that there exist no general and operational 3-D FEM tools that implement curved finite elements of higher geometrical orders that would enable accurate and efficient modeling of curvature.

This paper proposes a novel higher order (large-domain) Galerkin-type finite-element technique for 3-D electromagnetics based on higher order geometrical modeling and higher order field modeling, and presents its implementation in eigenvalue analysis of arbitrary 3-D inhomogeneous electromagnetic cavities. The volume elements adopted for the approximation of geometry are generalized curvilinear interpolatory hexahedra of arbitrary geometrical orders. The proposed basis functions for the approximation of fields within the elements are hierarchical curl-conforming polynomial vector basis functions of arbitrary orders. The elements are implemented for the geometrical orders from 1 to 4 and field-approximation orders from 1 to 10 in the same FEM method. The new technique enables excellent curvature modeling (e.g., a sphere is practically perfectly modeled by a single curved hexahedral finite element) and excellent field-distribution modeling (e.g., tenth-order polynomial field approximation in the three parametric coordinates in a hexahedral finite element). This enables using as large as approximately  $2\lambda \times 2\lambda \times 2\lambda$  curved FEM hexahedra as building blocks for modeling of the electromagnetic structure (which is 20 times the traditional low-order modeling discretization limit of  $\lambda/10$  in each dimension). Element orders in the model,

Manuscript received August 7, 2002; revised November 5, 2002.

The authors are with the Department of Electrical and Computer Engineering, University of Massachusetts Dartmouth, Dartmouth, MA 02747-2300 USA (e-mail: bnotaros@umassd.edu).

Digital Object Identifier 10.1109/TMTT.2003.808680

however, can also be low, so that the lower order modeling approach is actually included in the higher order modeling. Most importantly, since the proposed basis functions are hierarchical, a whole spectrum of element sizes (from a very small fraction of  $\lambda$  to  $2\lambda$ ), geometrical orders (from 1 to 4), and field-approximation orders (from 1 to 10) can be used at the same time in a single simulation model of a complex structure, making this method essentially a combined low-to-high-order method. Additionally, the technique provides a whole range of element shapes (e.g., brick-, slab-, and rod-like planar hexahedra, as well as spherically, cylindrically, and elliptically shaped curved hexahedra, and also other “irregular” and/or curved hexahedral shapes) to be used in a simulation model as well.

The one-dimensional (1-D) version of the new technique was presented in [19]. The preliminary results of 3-D eigenvalue analysis of rectangular air-filled metallic cavities for the higher order model with a single trilinear hexahedron (hexahedron of the first geometrical order) were presented in [20]. Similar (divergence-conforming) higher order basis functions in trilinear hexahedral volume elements have been used for the approximation of volume currents in the large-domain (entire-domain) volume-integral-equation Galerkin-type method of moments (MoM) [21]–[24]. A surface (boundary element) version of this method, using bilinear quadrilateral surface elements with twofold higher order divergence-conforming polynomial basis functions for the approximation of surface currents, has been used in the Galerkin-type large-domain MoM solution to surface integral equations [23]–[25].

Section II of this paper presents the mathematical background and numerical components of the new finite-element technique. This includes the generation of generalized curvilinear hexahedral elements for higher order modeling of geometry, implementation of hierarchical polynomial vector basis functions for higher order modeling of fields within the elements, and Galerkin testing procedure for discretizing the curl–curl electric-field vector-wave equation in the context of eigenvalue analysis of arbitrary electromagnetic cavities. In Section III, the efficiency, accuracy, and convergence of the higher order elements are evaluated and discussed for various geometries. The results obtained by the new FEM technique are compared with the analytical solutions and the numerical results obtained by low-order FEM techniques using small bricks, tetrahedra, and triangular prisms, respectively, as basic elements. Solutions obtained by means of the higher order FEM require significantly fewer unknowns (reduction by an order of magnitude) as compared to the solutions obtained by the low-order methods. The examples show excellent flexibility and efficiency of the presented finite elements at modeling of both field variation and curvature, and their excellent potential for  $p$ -refinement procedures.

## II. NOVEL HIGHER ORDER FINITE-ELEMENT TECHNIQUE FOR 3-D ELECTROMAGNETICS

As basic building blocks for geometrical modeling of 3-D electromagnetic structures of arbitrary shapes and material inhomogeneities, we adopt generalized curved parametric hexa-

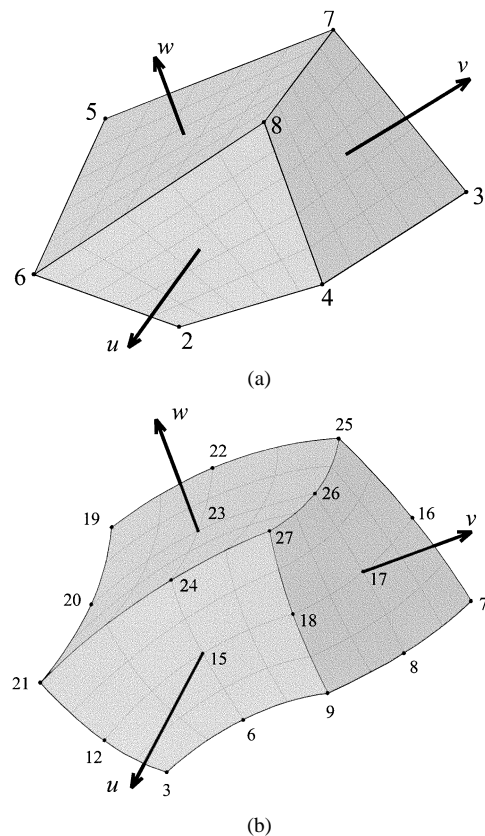


Fig. 1. Two simplest generalized hexahedra described by (1). (a) Trilinear hexahedron ( $K = 1$ ). (b) Triquadratic hexahedron ( $K = 2$ ).

hedra [2] of higher (theoretically arbitrary) geometrical orders. A generalized hexahedron is determined by  $M = (K + 1)^3$  points (interpolation nodes) arbitrarily positioned in space,  $K(K \geq 1)$  being the geometrical order of the element. It can be described analytically as

$$\mathbf{r}(u, v, w) = \sum_{i=1}^M \mathbf{r}_i \cdot p_i(u, v, w) = \sum_{m=0}^K \sum_{n=0}^K \sum_{l=0}^K \mathbf{a}_{mnl} u^m v^n w^l, \quad -1 \leq u, v, w \leq 1 \quad (1)$$

where  $\mathbf{r}_1, \mathbf{r}_2, \dots$ , and  $\mathbf{r}_M$  are the position vectors of the interpolation nodes,  $p_i(u, v, w)$  are Lagrange-type interpolation polynomials satisfying the Kronecker delta relation  $p_i(u_j, v_j, w_j) = \delta_{ij}$ , with  $u_j, v_j$ , and  $w_j$  representing the parametric coordinates of the  $j$ th node, and  $\mathbf{a}_{mnl}$  are constant vector coefficients related to  $\mathbf{r}_1, \mathbf{r}_2, \dots, \mathbf{r}_M$ . Shown in Fig. 1(a) is the first-order element ( $K = 1$ ), called the trilinear hexahedron [19]–[24], along with the visible coordinate lines. It is determined solely by  $M = 8$  interpolation points—its eight vertices. Its edges and all coordinate lines are straight, whereas its sides, so-called bilinear quadrilateral surfaces [23]–[25], are somewhat curved (inflexed). Note that even these hexahedra provide the same or better flexibility for geometrical modeling of general electromagnetic structures, as compared to commonly used elements in the form of bricks, tetrahedra, and triangular prisms. The second-order element ( $K = 2$ ), called the triquadratic hexahedron, shown in Fig. 1(b), is determined by  $M = 27$  interpolation points arbitrarily positioned in space.

Of course, parametric bodies of higher ( $K > 2$ ) geometrical orders provide additional flexibility and accuracy in modeling of complex curved structures. However, the use of flexible higher order curved elements is cost effective only if they can be made electrically large, which implies the use of higher order field expansions within the elements as well. Furthermore, in order to make the modeling of realistic structures optimal, it is convenient to have elements of different orders and sizes combined together in the same mesh. If both of these requirements are to be satisfied, implementation of hierarchical-type higher order polynomial basis functions for the approximation of fields is the right choice.

Our FEM formulation starts with the curl-curl electric-field vector-wave equation

$$\nabla \times \mu_r^{-1} \nabla \times \mathbf{E} - k_0^2 \epsilon_r \mathbf{E} = 0 \quad (2)$$

where  $\epsilon_r$  and  $\mu_r$  are complex relative permittivity and permeability of the inhomogeneous medium, respectively,  $\mathbf{E}$  is the electric-field complex intensity vector,  $k_0 = \omega \sqrt{\epsilon_0 \mu_0}$  is the free-space wavenumber, and  $\omega$  is the angular frequency of the implied time-harmonic variation. At material interfaces,  $\mathbf{E}$  must be tangentially continuous.

We represent the electric-field intensity vector inside every hexahedron as

$$\mathbf{E} = \sum_{i=0}^{N_u-1} \sum_{j=0}^{N_v} \sum_{k=0}^{N_w} \alpha_{uijk} \mathbf{f}_{uijk} + \sum_{i=0}^{N_u} \sum_{j=0}^{N_v-1} \sum_{k=0}^{N_w} \alpha_{vijk} \mathbf{f}_{vijk} + \sum_{i=0}^{N_u} \sum_{j=0}^{N_v} \sum_{k=0}^{N_w-1} \alpha_{wijk} \mathbf{f}_{wijk} \quad (3)$$

where  $\mathbf{f}$  are curl-conforming hierarchical-type vector basis functions defined by

$$\begin{aligned} \mathbf{f}_{uijk} &= u^i P_j(v) P_k(w) \mathbf{a}'_u \\ \mathbf{f}_{vijk} &= P_i(u) v^j P_k(w) \mathbf{a}'_v \\ \mathbf{f}_{wijk} &= P_i(u) P_j(v) w^k \mathbf{a}'_w \\ P_i(u) &= \begin{cases} 1 - u, & i = 0 \\ u + 1, & i = 1 \\ u^i - 1, & i \geq 2, \text{ even} \\ u^i - u, & i \geq 3, \text{ odd}, \\ -1 \leq u, v, w \leq 1. \end{cases} \end{aligned} \quad (4)$$

$N_u$ ,  $N_v$ , and  $N_w$  are the adopted degrees of the polynomial approximation, which are entirely independent of the element geometrical order  $K$  and  $\alpha_{uijk}$ ,  $\alpha_{vijk}$ , and  $\alpha_{wijk}$  are unknown field-distribution coefficients. The mixed-order arrangement of sum limits in (3) is in accordance with the reduced-gradient criterion [18], which is a preferable choice for modeling of waveguiding structures and 3-D resonant cavities, where the use of complete functions may lead to spurious solutions and incorrect results. The reciprocal unitary vectors  $\mathbf{a}'_u$ ,  $\mathbf{a}'_v$ , and  $\mathbf{a}'_w$  in (4) are obtained as

$$\begin{aligned} \mathbf{a}'_u &= \frac{\mathbf{a}_v \times \mathbf{a}_w}{J} \\ \mathbf{a}'_v &= \frac{\mathbf{a}_w \times \mathbf{a}_u}{J} \\ \mathbf{a}'_w &= \frac{\mathbf{a}_u \times \mathbf{a}_v}{J} \end{aligned} \quad (5)$$

where  $J$  is the Jacobian of the covariant transformation

$$J = (\mathbf{a}_u \times \mathbf{a}_v) \cdot \mathbf{a}_w. \quad (6)$$

The unitary vectors are given by

$$\mathbf{a}_u = \frac{d\mathbf{r}}{du} \quad \mathbf{a}_v = \frac{d\mathbf{r}}{dv} \quad \mathbf{a}_w = \frac{d\mathbf{r}}{dw} \quad (7)$$

with  $\mathbf{r}$  given in (1). The field expansions automatically satisfy continuity boundary conditions for tangential fields on surfaces shared by adjacent hexahedra in the model (curl-conforming functions). Note that similar higher order basis functions in the divergence-conforming form are used in conjunction with trilinear ( $K = 1$ ) hexahedra for the large-domain (entire-domain) MoM solution to volume integral equations [21]–[24]. Basis functions defined in (4) are hierarchical functions (each lower order set of functions is a subset of all higher order sets). They enable using different orders of field approximation in different elements, as well as in different directions within each element, which allows for a whole spectrum of element sizes (e.g., from a very small fraction of  $\lambda$  to a couple of  $\lambda$ ) and shapes to be used in a simulation model. Hierarchical basis functions, on the other hand, generally have poor orthogonality properties, which results in FEM matrices with large condition numbers. However, several approaches for improving the orthogonality of hierarchical higher order basis functions and the condition number of matrices in the context of both the FEM and MoM have been proposed to cope with this problem [13], [15], [26], [27].

Properties of the basis functions in (4) allow connection of any two elements regardless of the adopted geometrical orders, field-expansion orders, or local orientations. The only requirement that needs to be satisfied is the geometrical compatibility of the joint face. In our assembly procedure, the geometrical interpolation nodes associated with the two elements that govern the geometry of the common face are ordered in a way that ensures a symmetrical or antisymmetrical variation of the corresponding parametric coordinates. The continuity of the tangential field across the common face is enforced by equating the corresponding tangential-field coefficients associated with the elements, with additional corrections due to possibly different element orientations. The procedure has to be repeated for all faces shared by pairs of elements in the mesh. For elements with different geometrical orders, the same parametric presentations on both sides of the common face are ensured by placing the interpolation nodes of the element with a higher order at positions that match the parameter values already determined by the interpolation nodes of the element with a lower order. For elements with different field-expansion orders, the tangential-field coefficients are matched only up to the lesser of the corresponding orders and are set to zero for the remaining tangential-field basis functions. This order reduction pertains to the common face only and does not influence the expansions throughout the rest of the volumes of the elements.

According to the Galerkin testing procedure, weighted residuals of (2) are formed as

$$\int_V \mathbf{f}_{ijk} \cdot \nabla \times \mu_r^{-1} \nabla \times \mathbf{E} dV - k_0^2 \int_V \epsilon_r \mathbf{f}_{ijk} \cdot \mathbf{E} dV = 0 \quad (8)$$

where  $V$  is the volume of a generalized hexahedron and  $\mathbf{f}_{\hat{i}\hat{j}\hat{k}}$  stands for any of the functions  $\mathbf{f}_{u\hat{i}\hat{j}\hat{k}}$ ,  $\mathbf{f}_{v\hat{i}\hat{j}\hat{k}}$ , or  $\mathbf{f}_{w\hat{i}\hat{j}\hat{k}}$ . The first integral in (8) is then transformed by employing the vector analog to Green's first identity, which yields the weak form representation of (2) suitable for numerical solution. Finally, the boundary conditions are imposed over the boundary surface of the entire FEM domain, providing a numerical interface between the FEM domain and remaining space. In analysis of metallic cavities, however, these conditions reduce to the requirement that the tangential component of  $\mathbf{E}$  vanish near the cavity walls, which is the simplest mesh termination technique and is easily enforced by *a priori* setting to zero the field-distribution coefficients associated with the tangential  $\mathbf{E}$  on the sides (generalized quadrilateral surfaces) of elements adjacent to cavity walls. This leads to the following generalized eigenvalue problem:

$$[A]\{\alpha\} = k_0^2[B]\{\alpha\} \quad (9)$$

where  $k_0^2$  are the eigenvalues of the system. The elements of matrices  $[A]$  and  $[B]$  corresponding to  $u$ -components of the field expansion and testing are given by

$$UU_{\hat{i}\hat{j}\hat{k}i\hat{j}\hat{k}} = \int_V \mu_r^{-1} (\nabla \times \mathbf{f}_{u\hat{i}\hat{j}\hat{k}}) \cdot (\nabla \times \mathbf{f}_{u\hat{i}\hat{j}\hat{k}}) dV$$

and

$$UB_{\hat{i}\hat{j}\hat{k}i\hat{j}\hat{k}} = \int_V \varepsilon_r \mathbf{f}_{u\hat{i}\hat{j}\hat{k}} \cdot \mathbf{f}_{u\hat{i}\hat{j}\hat{k}} dV \quad (10)$$

respectively, with analogous expressions for the elements corresponding to other combinations of field components. Starting from (4), the curl of the function  $\mathbf{f}_{u\hat{i}\hat{j}\hat{k}}$  can be found as [10]

$$\nabla \times \mathbf{f}_{u\hat{i}\hat{j}\hat{k}} = \frac{1}{J} \left[ u^i P_j(v) \frac{dP_k(w)}{dw} \mathbf{a}_v - u^i \frac{dP_j(v)}{dv} P_k(w) \mathbf{a}_w \right] \quad (11)$$

and analogous expressions hold for functions  $\mathbf{f}_{v\hat{i}\hat{j}\hat{k}}$  and  $\mathbf{f}_{w\hat{i}\hat{j}\hat{k}}$ . This simplifies the evaluation of  $A$ -integrals in (10), whereas  $B$ -integrals can readily be evaluated in their present form. All integrals are integrated numerically in the  $u-v-w$  domain as

$$\int_V F(u, v, w) dV = \int_u \int_v \int_w F(u, v, w) J du dv dw \quad (12)$$

and the integration is carried out using the Gauss-Legendre threefold integration formula in  $(10 + N_u) \times (10 + N_v) \times (10 + N_w)$  points. The system in (9) is solved for all eigenvalues using a standard eigenvalue solver.

### III. NUMERICAL RESULTS AND DISCUSSION

As the first example, consider a rectangular air-filled metallic cavity with dimensions 1 cm  $\times$  0.5 cm  $\times$  0.75 cm. Shown in Table I(a) are the percentage errors of the resonant-mode wavenumbers  $k_0$  computed by the higher order FEM and those obtained by low-order FEM techniques using small triangular prisms [5], bricks [4], and tetrahedra [4], respectively, as basic elements, as well as the technique using a linear tangential/quadratic normal (LT/QN) field representation

TABLE I  
ERROR OF  $k_0$  FOR THE EIGENVALUE ANALYSIS OF A RECTANGULAR CAVITY (1 cm  $\times$  0.5 cm  $\times$  0.75 cm). (a) COMPARISON OF A HIGHER ORDER SINGLE-ELEMENT FEM AND FOUR REFERENCE FEM SOLUTIONS. (b) CONVERGENCE OF THE HIGHER ORDER SINGLE-ELEMENT FEM WITH INCREASING THE FIELD EXPANSION POLYNOMIAL ORDERS

| Mode              | $k_0$ [cm <sup>-1</sup> ]<br>(Exact) | Error  [%]                    |                               |                                   |                              |                                |
|-------------------|--------------------------------------|-------------------------------|-------------------------------|-----------------------------------|------------------------------|--------------------------------|
|                   |                                      | Prisms [5]<br>382<br>Unknowns | Bricks [4]<br>270<br>Unknowns | Tetrahedra [4]<br>260<br>Unknowns | LT/QN [9]<br>204<br>Unknowns | Higher-order<br>29<br>Unknowns |
| TE <sub>101</sub> | 5.236                                | 0.73                          | 1.36                          | 0.44                              | 0.54                         | 0.42                           |
| TM <sub>110</sub> | 7.025                                | 2.32                          | 2.23                          | 0.70                              | 0.57                         | 0.53                           |
| TE <sub>011</sub> | 7.551                                | 0.53                          | 2.58                          | 1.00                              | 0.18                         | 0.66                           |
| TE <sub>201</sub> | 7.551                                | 0.64                          | 3.13                          | 0.56                              | 1.89                         | 2.38                           |
| TM <sub>111</sub> | 8.179                                | 0.22                          | 2.09                          | 2.29                              | 0.56                         | 0.56                           |
| TE <sub>111</sub> | 8.179                                |                               | 2.09                          | 0.70                              | 1.57                         | 0.56                           |
| TM <sub>210</sub> | 8.886                                |                               | 2.98                          | 3.53                              | 0.84                         | 1.91                           |
| TE <sub>102</sub> | 8.947                                |                               | 5.38                          | 1.70                              | 0.49                         | 2.76                           |

(a)

| Mode              | $k_0$ [cm <sup>-1</sup> ]<br>(Exact) | Error  [%]<br>Higher-order FEM |                 |                 |
|-------------------|--------------------------------------|--------------------------------|-----------------|-----------------|
|                   |                                      | 29<br>Unknowns                 | 240<br>Unknowns | 756<br>Unknowns |
| TE <sub>101</sub> | 5.236                                | 0.42                           | 0.74 $10^{-3}$  | 0.17 $10^{-6}$  |
| TM <sub>110</sub> | 7.025                                | 0.53                           | 0.74 $10^{-3}$  | 0.17 $10^{-6}$  |
| TE <sub>011</sub> | 7.551                                | 0.66                           | 0.74 $10^{-3}$  | 0.17 $10^{-6}$  |
| TE <sub>201</sub> | 7.551                                | 2.38                           | 0.20 $10^{-1}$  | 0.49 $10^{-4}$  |
| TM <sub>111</sub> | 8.179                                | 0.56                           | 0.74 $10^{-3}$  | 0.17 $10^{-6}$  |
| TE <sub>111</sub> | 8.179                                | 0.56                           | 0.74 $10^{-3}$  | 0.17 $10^{-6}$  |
| TM <sub>210</sub> | 8.886                                | 1.91                           | 0.15 $10^{-1}$  | 0.35 $10^{-4}$  |
| TE <sub>102</sub> | 8.947                                | 2.76                           | 0.26 $10^{-1}$  | 0.62 $10^{-4}$  |

(b)

on tetrahedra [9]. In the higher order FEM approach, the cavity is modeled by a single trilinear hexahedral element (which, in this case, reduces to a brick) and only 29 unknowns ( $N_u = 4, N_v = 2, N_w = 3$ ). Note that this is literally an entire-domain FEM model (an entire computational domain is represented by a single finite element). It can be observed that, for the same level of accuracy, solutions obtained by means of the higher order FEM require significantly fewer unknowns, as compared to the solutions obtained by the other four methods (29 compared to 382, 270, 260, and 204, respectively). Table I(b) shows a very good convergence of the higher order FEM with increasing the field-expansion polynomial orders to  $N_u = N_v = N_w = 5$  and  $N_u = N_v = N_w = 7$ , which corresponds to a  $p$ -refinement of the model, the respective total numbers of unknowns being 240 and 756.

The next example is a cubical air-filled metallic cavity of 0.5 cm on a side. Fig. 2 shows a plot of the percentage error in calculating  $k_0$  of the dominant degenerate eigenmodes against the number of unknowns for the low-order FEM models with small rectangular bricks [4] and small tetrahedra [4] and three higher order models. In the first higher order solution, the cavity is represented by a single (entire-domain) trilinear hexahedron with the field-expansion polynomial orders being varied from  $N_u = N_v = N_w = 2$  to  $N_u = N_v = N_w = 7$  ( $p$ -refinement). The other two higher order solutions, using eight-element and 27-element uniform meshes, are shown to indicate the model behavior when the number of elements is increased as well,

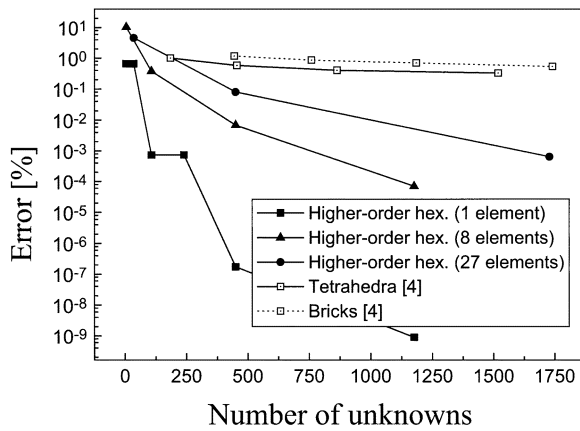


Fig. 2. Percentage error in calculating  $k_0$  of the dominant degenerate eigenmodes of a cubical air-filled metallic cavity of 0.5 cm on a side against the number of unknowns for three higher order FEM models (with 1, 8, and 27 hexahedra) and two low-order FEM models (with small tetrahedra and bricks).

which corresponds to an  $h$ -refinement of the model. We observe great superiority of higher order FEM solutions over low-order ones. We also note that finer higher order meshes result in a worse accuracy to number-of-unknowns ratio as compared to coarser meshes in this example. Generally, optimal modeling is achieved by keeping the elements as large as possible—of course, within certain limits. Based on many numerical experiments, we have adopted  $2\lambda$  to be the maximal dimension of finite elements and the general limit in the FEM procedure beyond which the structure is subdivided into smaller, but still large-domain optimal elements (note that the corresponding low-order FEM limit is  $0.1\lambda$ ). The same limit holds for higher order MoM modeling [24].

Somewhat more complex cavities are now analyzed. First, consider a half-filled  $1 \text{ cm} \times 0.1 \text{ cm} \times 1 \text{ cm}$  rectangular metallic cavity with a dielectric filling of relative permittivity  $\epsilon_r = 2$  extending from  $z = 0.5 \text{ cm}$  to  $z = 1 \text{ cm}$  (Fig. 3). Percentage errors in computation of  $k_0$  for the first six modes are shown in Table II. The results obtained by the higher order FEM using two trilinear hexahedral finite elements, as indicated in Fig. 3, are compared against a low-order tetrahedral-mesh FEM solution [4]. The number of unknowns in the higher order model is kept by roughly an order of magnitude smaller than that with the low-order model, and excellent accuracy is achieved. The exact numbers of unknowns and field-approximation polynomial orders used in both higher order hexahedra for different modes are also given in Table II.

Next, consider an empty rectangular cavity with a metallic ridge, shown in Fig. 4. Table III shows the computed results for the free-space wavenumbers  $k_0$  of the cavity (there is no exact analytical solution to this problem). Two higher order solutions are presented with the cavity modeled by three and five trilinear hexahedra, shown in Fig. 5(a) and (b), and the resulting total numbers of unknowns 68 and 81, respectively. The adopted field-approximation polynomial orders in individual directions are indicated in this figure. Shown in Table III are also the results obtained by two low-order tetrahedral-mesh FEM models [4] with 267 and 671 unknowns, respectively. A good agreement between the higher order and low-order FEM

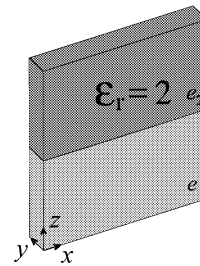


Fig. 3. Half-filled  $1 \text{ cm} \times 0.1 \text{ cm} \times 1 \text{ cm}$  rectangular cavity modeled by two trilinear hexahedral finite elements.

TABLE II  
PERCENTAGE ERROR OF  $k_0$  FOR THE CAVITY IN FIG. 3. A HIGHER ORDER TWO-ELEMENT SOLUTION AND A LOW-ORDER TETRAHEDRAL-MESH SOLUTION

| Mode               | Exact $k_0$ [cm <sup>-1</sup> ] | Error  [%]              |                             | Numerical parameters of the higher-order model |                      |
|--------------------|---------------------------------|-------------------------|-----------------------------|--|----------------------|
|                    |                                 | Tetrahedra [4] Unknowns | Higher-order 20-25 Unknowns | Exact Number of Unknowns                       | Orders $N_x-N_y-N_z$ |
| TE <sub>Z101</sub> | 3.538                           | 0.11                    | 0.004                       | 21   | 4-1-4                |
| TE <sub>Z201</sub> | 5.445                           | 0.10                    | 0.04                        | 20   | 5-1-3                |
| TE <sub>Z102</sub> | 5.935                           | 0.32                    | 1.07                        | 21   | 4-1-4                |
| TE <sub>Z301</sub> | 7.503                           | 0.04                    | 0.2                         | 25   | 6-1-3                |
| TE <sub>Z203</sub> | 7.633                           | 0.97                    | 0.9                         | 25   | 6-1-3                |
| TE <sub>Z103</sub> | 8.096                           | 0.50                    | 0.58                        | 21   | 4-1-4                |

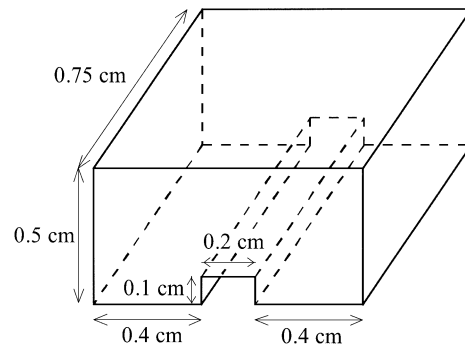


Fig. 4. Air-filled rectangular cavity with a metallic ridge.

TABLE III  
COMPUTED  $k_0$  FOR THE CAVITY IN FIG. 4. TWO HIGHER ORDER HEXAHEDRAL-MESH SOLUTIONS [MODELS IN FIG. 5(a) AND (b)] AND TWO LOW-ORDER TETRAHEDRAL-MESH SOLUTIONS

| Mode No. | Calculated $k_0$ [cm <sup>-1</sup> ] |              |                  |             |
|----------|--------------------------------------|--------------|------------------|-------------|
|          | Tetrahedra [4]                       |              | Higher-order FEM |             |
|          | 267 Unknowns                         | 671 Unknowns | 68 Unknowns      | 81 Unknowns |
| 1        | 4.941                                | 4.999        | 5.083            | 5.088       |
| 2        | 7.284                                | 7.354        | 7.572            | 7.471       |
| 3        | 7.691                                | 7.832        | 8.207            | 7.903       |
| 4        | 7.855                                | 7.942        | 8.479            | 7.967       |
| 5        | 8.016                                | 7.959        | 8.743            | 8.019       |
| 6        | 8.593                                | 8.650        | 9.108            | 9.001       |
| 7        | 8.906                                | 8.916        | 9.458            | 9.111       |
| 8        | 9.163                                | 9.103        | 10.04            | 9.169       |
| 9        | 9.679                                | 9.757        | 10.22            | 10.08       |
| 10       | 9.837                                | 9.927        | 10.69            | 10.37       |

results is observed; the reduction of the number of unknowns with the higher order FEM again being by up to an order of magnitude when compared to the low-order FEM. We note

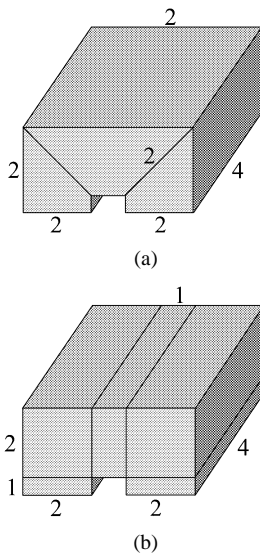


Fig. 5. (a) Three- and (b) five-element higher order FEM hexahedral models of the cavity in Fig. 4. The adopted field-approximation polynomial orders in individual directions are also indicated.

also a very effective three-element hexahedral FEM modeling of this nonstandard shape in the mesh in Fig. 5(a). However, the five-element model in Fig. 5(b) provides better accuracy at predicting the fields in the vicinity of the ridge and better overall accuracy of the results.

As an example of higher order FEM modeling of curved structures, Table IV(a) and (b) show the percentage error in calculating  $k_0$  for first several modes of an empty spherical cavity (1 cm in radius). The sphere is modeled by a single (entire-domain) curved hexahedron of the second ( $K = 2$ ) geometrical order [see Table IV (a)] and fourth ( $K = 4$ ) geometrical order [see Table IV (b)], respectively, and field-approximation orders are varied from  $N_u = N_v = N_w = 3$  to  $N_u = N_v = N_w = 6$  in both solutions ( $p$ -refinement). The results are compared with a low-order tetrahedral mesh FEM model [4]. We observe that the second-order geometrical approximation [see Table IV(a)] with only 108 unknowns (64% less than with the low-order model) yields very good results for the first eight modes. The  $p$ -refinement improves the results for all modes, whereas an inherent geometrical error is always present. A considerable increase in accuracy for all modes is observed when the curved hexahedron of the fourth geometrical order is used [see Table IV(b)]. Note that, here, as low as only 36 unknowns suffice for the analysis of lower modes.

Shown in Fig. 6 is the comparison of the convergence of the results for the dominant mode  $k_0$  of a spherical cavity (1 m in radius) with an increase in the number of unknowns for the two higher order models with a single curved hexahedron (field-expansion orders are varied from 3 to 7 in all directions) and a low-order tetrahedral-mesh solution [6]. This figure demonstrates great numerical advantages of the higher order FEM over the low-order FEM in this case; the number of unknowns for 1% accuracy with the low-order model (1840) being 17 times that (108) with both higher order models. We again observe a significant additional improvement in accuracy as a result of using geometrical modeling of the fourth-order instead of the second-order geometrical modeling. In other words, it is impos-

TABLE IV  
ERROR OF  $k_0$  COMPARISON FOR THE EIGENVALUE ANALYSIS OF AN AIR-FILLED SPHERICAL CAVITY, 1 cm IN RADIUS. (a) HIGHER ORDER SINGLE-ELEMENT FEM MODELING WITH SECOND-ORDER GEOMETRICAL APPROXIMATION AND (b) FOURTH-ORDER GEOMETRICAL APPROXIMATION, AND A LOW-ORDER TETRAHEDRAL-MESH FEM SOLUTION

| Mode                   | Exact $k_0$<br>[cm <sup>-1</sup> ] | Error  [%]     |  |      |      |      |
|------------------------|------------------------------------|----------------|--|------|------|------|
|                        |                                    | Tetrahedra [4] | Higher-order FEM with 2 <sup>nd</sup> order geometry |      |      |      |
| Unknowns               |                                    | 300            | 36   | 108  | 240  | 450  |
| TM <sub>010</sub>      | 2.744                              | 2.04           | 4.60   | 1.00 | 0.94 | 0.91 |
| TM <sub>111,even</sub> |                                    | 2.11           | 4.60   | 1.00 | 0.94 | 0.91 |
| TM <sub>111,odd</sub>  |                                    | 2.44           | 4.60   | 1.00 | 0.94 | 0.91 |
| TM <sub>021</sub>      | 3.870                              | 2.02           | 6.85   | 1.39 | 0.89 | 0.85 |
| TM <sub>121,even</sub> |                                    | 2.99           | 6.85   | 1.39 | 0.89 | 0.85 |
| TM <sub>121,odd</sub>  |                                    | 3.20           | 6.85   | 4.47 | 0.89 | 0.85 |
| TM <sub>221,even</sub> |                                    | 4.34           | 15.57  | 4.47 | 1.39 | 1.09 |
| TM <sub>221,odd</sub>  |                                    | 4.59           | 15.57  | 4.47 | 1.39 | 1.09 |
| TE <sub>011</sub>      | 4.493                              | 1.33           | 11.38  | 7.30 | 1.19 | 1.09 |
| TE <sub>111,even</sub> |                                    | 0.47           | 11.38  | 7.30 | 1.19 | 1.09 |
| TE <sub>111,odd</sub>  |                                    | 1.25           | 11.38  | 7.30 | 1.19 | 1.09 |

(a)

| Mode                   | Exact $k_0$<br>[cm <sup>-1</sup> ] | Error  [%]     |  |       |        |      |
|------------------------|------------------------------------|----------------|--|-------|--------|------|
|                        |                                    | Tetrahedra [4] | Higher-order FEM with 4 <sup>th</sup> order geometry |       |        |      |
| Unknowns               |                                    | 300            | 36   | 108   | 240    | 450  |
| TM <sub>010</sub>      | 2.744                              | 2.04           | 2.79   | 0.78  | 0.10   | 0.25 |
| TM <sub>111,even</sub> |                                    | 2.11           | 2.79   | 0.78  | 0.10   | 0.25 |
| TM <sub>111,odd</sub>  |                                    | 2.44           | 2.79   | 0.78  | 0.10   | 0.25 |
| TM <sub>021</sub>      | 3.870                              | 2.02           | 3.40   | 0.088 | 0.0067 | 0.02 |
| TM <sub>121,even</sub> |                                    | 2.99           | 3.40   | 0.088 | 0.0067 | 0.02 |
| TM <sub>121,odd</sub>  |                                    | 3.20           | 3.40   | 0.44  | 0.0067 | 0.02 |
| TM <sub>221,even</sub> |                                    | 4.34           | 7.84   | 0.44  | 0.093  | 0.23 |
| TM <sub>221,odd</sub>  |                                    | 4.59           | 7.84   | 0.44  | 0.093  | 0.23 |
| TE <sub>011</sub>      | 4.493                              | 1.33           | 4.21   | 3.79  | 1.08   | 0.28 |
| TE <sub>111,even</sub> |                                    | 0.47           | 4.21   | 3.79  | 1.08   | 0.28 |
| TE <sub>111,odd</sub>  |                                    | 1.25           | 4.21   | 3.79  | 1.08   | 0.28 |

(b)

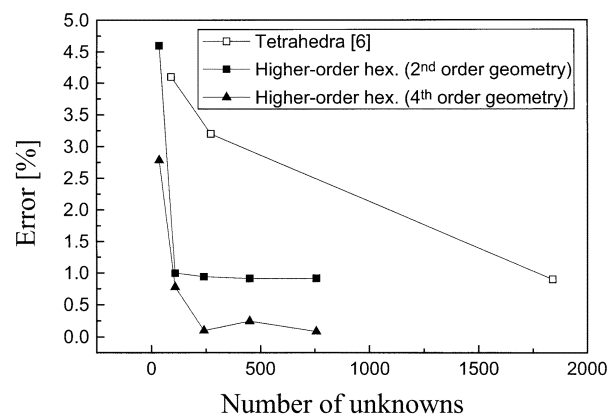


Fig. 6. Comparison of two higher order FEM solutions (single-element models of the second and fourth geometrical orders) and a low-order tetrahedral-mesh solution for the dominant mode  $k_0$  of a spherical cavity (1 m in radius) against the number of unknowns.

sible to  $p$ -refine the higher order model with the second geometrical order below approximately 1% error in calculating  $k_0$  due

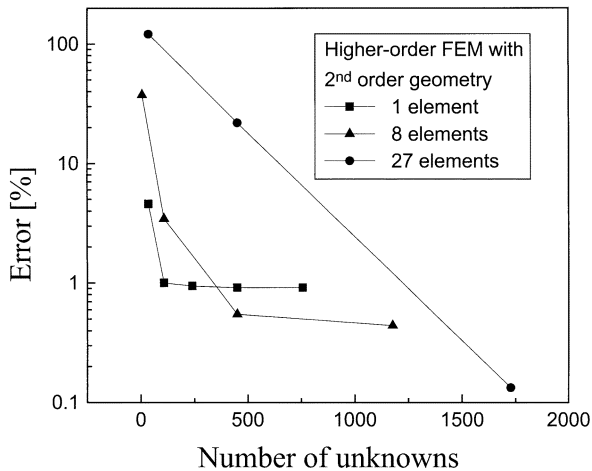


Fig. 7. Percentage error in higher order FEM computation of the dominant mode  $k_0$  for a spherical cavity, modeled by one, eight, and 27 triquadratic ( $K = 2$ ) hexahedral elements with the field-approximation polynomial orders ranging from 2 to 6, 1 to 4, and 1 to 3, respectively, in all three parametric coordinates within individual elements.

to the inherent geometrical error of the model, whereas the  $p$ -refinement in the model with the fourth geometrical order brings the analysis error quickly down to a fraction of a percent.

We notice a nonmonotonic (oscillating) error decrease in the low-error region with the fourth-order geometrical model in Fig. 6 [see also Table IV(b)]. This oscillation falls in the error margin for the particular mode and the particular numerical discretization of field equations in this example. However, the average error for all calculated modes in Table IV(b) that corresponds to the points for the fourth-order model in Fig. 6 is 4.3%, 1.4%, 0.34%, 0.19%, and 0.15%, respectively. Note that this (or similar) average error, which indeed decreases monotonically when using  $p$ -refinement, is actually relevant for “dialing” accuracy, i.e., for determining minimal field expansion orders needed for the specified level of desired accuracy or acceptable uncertainty of the results, in practical implementations.

To further investigate numerical properties of different higher order models of a sphere, we show in Fig. 7 the comparison of the results in calculating the dominant mode  $k_0$  for a spherical cavity, modeled by one, eight, and 27 triquadratic ( $K = 2$ ) hexahedral elements, with the field-approximation polynomial orders being varied from 2 to 6, 1 to 4, and 1 to 3, respectively, in all directions. The models with eight and 27 elements correspond to the combined  $hp$ -refinement of the solution. We observe the following: for obtaining a 1%-accuracy solution, the single-element model is optimal (in terms of the required number of unknowns); 0.5% accuracy, however, cannot be achieved by a single-element model (of the second geometrical order) and  $p$ -refinement alone, but  $h$ -refinement (eight-element model) has to be employed as well. Finally, if 0.1% accuracy is desired, further  $hp$ -refinement with a 27-element model is needed. On the other hand, we also note that approximately 0.1% accuracy can be achieved using as little as 240 unknowns with a single-element model of the fourth geometrical order (see Fig. 6), whereas over 1728 unknowns and at least 27 elements are necessary for

getting the same level of accuracy if elements of the second geometrical order (triquadratic hexahedra) are used (Fig. 7).

#### IV. CONCLUSIONS

This paper has proposed a novel higher order finite-element technique for 3-D microwave modeling and has presented its implementation in eigenvalue analysis of arbitrary 3-D electromagnetic cavities. The technique represents a Galerkin-type method employing hierarchical curl-conforming vector basis functions of higher (1–10) polynomial orders defined in generalized curved hexahedra of higher (1–4) geometrical orders. The elements can be as large as approximately  $2\lambda \times 2\lambda \times 2\lambda$  (which is 20 times the traditional low-order modeling discretization limit of  $\lambda/10$  in each dimension). The new technique enables excellent field-distribution modeling. It has been demonstrated that entire rectangular and spherical cavities can be very accurately modeled by a single large hexahedral finite element with polynomial field-approximation basis functions of high orders. The method also enables excellent curvature modeling. It has been demonstrated that a sphere, which is customarily taken as an example of difficulties with modeling of curvature by many researchers, can be equally efficiently modeled as a cube. The flexibility of the new technique has allowed for a very effective modeling of a cavity with a dielectric loading and a cavity with a metallic ridge by means of only a few large finite elements. All the examples have shown excellent properties of higher order finite elements in the context of the  $p$ -refinement of solutions for models with both flat and curved surfaces. The results obtained by the higher order FEM are compared with the analytical solutions and with the numerical results obtained by different low-order FEM techniques, which utilize electrically small triangular prisms, bricks, and tetrahedra, respectively, as finite elements. It has been observed that the presented technique offers considerably improved accuracy, as well as significantly faster convergence as the number of unknowns increases. The reduction in the number of unknowns is by an order of magnitude when compared to low-order solutions.

#### REFERENCES

- [1] J. M. Jin, *The Finite Element Method in Electromagnetics*. New York: Wiley, 1993.
- [2] P. P. Silvester and R. L. Ferrari, *Finite Elements for Electrical Engineers*. Cambridge, U.K.: Cambridge Univ. Press, 1996.
- [3] J. L. Volakis, A. Chatterjee, and L. C. Kempel, *Finite Element Method for Electromagnetics*. Piscataway, NJ: IEEE Press, 1998.
- [4] A. Chatterjee, J. M. Jin, and J. L. Volakis, “Computation of cavity resonances using edge-based finite elements,” *IEEE Trans. Microwave Theory Tech.*, vol. 40, pp. 2106–2108, Nov. 1992.
- [5] T. Ozdemir and J. L. Volakis, “Triangular prisms for edge-based vector finite element analysis of conformal antennas,” *IEEE Trans. Antennas Propagat.*, vol. 45, pp. 788–797, May 1997.
- [6] J. S. Wang and N. Ida, “Eigenvalue analysis in electromagnetic cavities using divergence free finite elements,” *IEEE Trans. Magn.*, vol. 27, pp. 3978–3981, Sept. 1991.
- [7] —, “Curvilinear and higher order “edge” finite elements in electromagnetic field computation,” *IEEE Trans. Magn.*, vol. 29, pp. 1491–1493, Mar. 1993.
- [8] T. V. Yioultis and T. D. Tsiboukis, “Development and implementation of second and third order vector finite elements in various 3-D electromagnetic field problems,” *IEEE Trans. Magn.*, vol. 33, pp. 1812–1815, Mar. 1997.

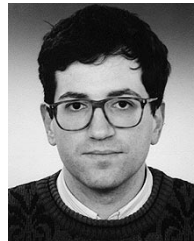
- [9] J. S. Savage and A. F. Peterson, "Higher order vector finite elements for tetrahedral cells," *IEEE Trans. Microwave Theory Tech.*, vol. 44, pp. 874–879, June 1996.
- [10] R. D. Graglia, D. R. Wilton, and A. F. Peterson, "Higher order interpolatory vector bases for computational electromagnetics," *IEEE Trans. Antennas Propagat.*, vol. 45, pp. 329–342, Mar. 1997.
- [11] L. S. Andersen and J. L. Volakis, "Development and application of a novel class of hierarchical tangential vector finite elements for electromagnetics," *IEEE Trans. Antennas Propagat.*, vol. 47, pp. 112–120, Jan. 1999.
- [12] —, "Accurate and efficient simulation of antennas using hierarchical mixed-order tangential vector finite elements for tetrahedra," *IEEE Trans. Antennas Propagat.*, vol. 47, pp. 1240–1243, Aug. 1999.
- [13] —, "Condition numbers for various FEM matrices," *J. Electromagn. Waves Applicat.*, vol. 13, pp. 1663–1679, 1999.
- [14] J. Wang and J. P. Webb, "Hierarchical vector boundary elements and  $p$ -adaptation for 3-D electromagnetic scattering," *IEEE Trans. Antennas Propagat.*, vol. 45, pp. 1869–1879, Dec. 1997.
- [15] J. P. Webb, "Hierarchical vector basis functions of arbitrary order for triangular and tetrahedral finite elements," *IEEE Trans. Antennas Propagat.*, vol. 47, pp. 1244–1253, Aug. 1999.
- [16] Z. Huang and J. P. Webb, "Iterative solvers for hierarchical vector finite element analysis of microwave problems," *IEEE Trans. Magn.*, vol. 37, pp. 3285–3288, Sept. 2001.
- [17] J. Liu and J.-M. Jin, "A novel hybridization of higher order finite element and boundary integral methods for electromagnetic scattering and radiation problems," *IEEE Trans. Antennas Propagat.*, vol. 49, pp. 1794–1806, Dec. 2001.
- [18] J. C. Nedelec, "Mixed finite elements in  $R_3$ ," *Numer. Math.*, vol. 35, pp. 315–341, 1980.
- [19] M. M. Ilić and B. M. Notaros, "Trilinear hexahedral finite elements with higher-order polynomial field expansions for hybrid SIE/FE large-domain electromagnetic modeling," in *IEEE AP-S Int. Symp. Dig.*, Boston, MA, July 8–13, 2001, pp. III.192–III.195.
- [20] —, "Computation of 3-D electromagnetic cavity resonances using hexahedral vector finite elements with hierarchical polynomial basis functions," in *IEEE AP-S Int. Symp. Dig.*, San Antonio, TX, June 16–21, 2002, pp. IV.682–685.
- [21] B. M. Notaros and B. D. Popovic, "General entire-domain method for analysis of dielectric scatterers," *Proc. Inst. Elect. Eng.*, pt. H, vol. 143, no. 6, pp. 498–504, Dec. 1996.
- [22] —, "General entire-domain Galerkin method for analysis of wire antennas in the presence of dielectric bodies," *Proc. Inst. Elect. Eng.*, pt. H, vol. 145, no. 1, pp. 13–18, Feb. 1998.
- [23] —, "Large-domain integral-equation method for analysis of general 3D electromagnetic structures," *Proc. Inst. Elect. Eng.*, pt. H, vol. 145, no. 6, pp. 491–495, December 1998.
- [24] B. M. Notaros, B. D. Popovic, J. P. Weem, R. A. Brown, and Z. Popovic, "Efficient large-domain MoM solution to electrically large practical EM problems," *IEEE Trans. Microwave Theory Tech.*, vol. 49, pp. 151–159, Jan. 2001.

- [25] B. D. Popovic and B. M. Kolundzija, *Analysis of Metallic Antennas and Scatterers*, ser. Electromagn. Wave Series 38. London, U.K.: IEE Press, 1994.
- [26] M. Djordjevic and B. M. Notaros, "Three types of higher-order MoM basis functions automatically satisfying current continuity conditions," in *IEEE AP-S Int. Symp. Dig.*, San Antonio, TX, June 16–21, 2002, pp. 610–613.
- [27] E. Jorgensen, J. L. Volakis, P. Meincke, and O. Breinbjerg, "Higher order hierarchical Legendre basis functions for iterative integral equation solvers with curvilinear surface modeling," in *IEEE AP-S Int. Symp. Dig.*, San Antonio, TX, June 16–21, 2002, pp. IV.618–621.



**Milan M. Ilić (S'00)** was born in Belgrade, Yugoslavia, in June 1970. He received the Dipl.Eng. and M.S. degrees in electrical engineering from the University of Belgrade, Belgrade, Yugoslavia, in 1995 and 2000, respectively, and is currently working toward the Ph.D. degree at the University of Massachusetts Dartmouth.

From 1995 to 2000, he was a Research and Teaching Assistant with the School of Electrical Engineering, University of Belgrade. His research interests include CEM, antennas, and passive microwave components and circuits.



**Branislav M. Notaroš (M'00)** was born in Zrenjanin, Yugoslavia, in 1965. He received the Dipl.Eng. (B.Sc.), M.Sc., and Ph.D. degrees in electrical engineering from the University of Belgrade, Belgrade, Yugoslavia, in 1988, 1992, and 1995, respectively.

He is currently an Assistant Professor of electrical and computer engineering with the University of Massachusetts Dartmouth. From 1996 to 1998, he was an Assistant Professor with the Department of Electrical Engineering, University of Belgrade. He spent the 1998–1999 academic year as a Visiting Research Associate with the University of Colorado at Boulder. His teaching activities are in the area of theoretical and applied electromagnetics. He is the Director of the Telecommunications Laboratory, Advanced Technology and Manufacturing Center, University of Massachusetts Dartmouth. He has authored or coauthored 12 journal papers, 33 conference papers, a book chapter, and three university workbooks. His research interests are predominantly in CEM and antenna design.

Dr. Notaroš was the recipient of the 1999 Institution of Electrical Engineers (IEE) Marconi Premium.